

自由飞行空间机器人的遥操作分数阶PID控制

时中^{1†}, 黄学祥¹, 谭谦¹, 胡天健^{1,2}

(1. 北京跟踪与通信技术研究所, 北京 100094; 2. 清华大学 航天航空学院, 北京 100084)

摘要: 作为空间操控的重要手段, 空间遥操作将趋向于更精细和更灵活. 然而传统的空间遥操作控制方法难以兼顾操作的精细性和灵活性. 针对这一问题, 本文阐述了一种面向自由飞行空间机器人的遥操作分数阶PID控制方法. 首先根据自由飞行空间机器人的动力学模型, 设计了空间遥操作分数阶PID控制系统. 其次, 针对空间遥操作时滞系统和系统的鲁棒性和抗干扰性要求, 基于系统的参数稳定域, 对分数阶PID控制器的参数进行整定. 最后, 数值仿真和地面遥操作实验验证了分数阶PID控制器的跟踪性能、抗干扰性、鲁棒性和抗时延抖动性能. 因此, 本文设计的分数阶PID控制器不仅适合于空间遥操作复杂时滞系统, 而且可以满足未来空间遥操作任务的发展需求.

关键词: 空间遥操作; PID控制; 分数阶微积分; 参数稳定域; D-分割法

中图分类号: V476.5 TP273 文献标识码: A

Fractional-order PID control for teleoperation of a free-flying space robot

SHI Zhong^{1†}, HUANG Xue-xiang¹, TAN Qian¹, HU Tian-jian^{1,2}

(1. Beijing Institute of Tracking and Telecommunications Technology, Beijing 100094, China;
2. School of Aerospace Engineering, Tsinghua University, Beijing 100084, China)

Abstract: As one of the most important ways of executing tasks of space operations, space teleoperation will develop to be “more careful and more flexible” in the future. However, the conventional control method for space teleoperation has difficulty in balancing the precision and flexibility of operations. Aiming at this problem, this paper presents a fractional-order PID (FOPID) control method for teleoperation of a free-flying space robot. First, based on the dynamic model of the free-flying space robot, the FOPID control system for space teleoperation is designed. Then, directing to the space teleoperation time-delay system and the requirements of the robustness and anti-interference capabilities for space teleoperation, the parameters of FOPID controller are tuned based on its stability domain. Finally, numerical simulation and ground teleoperation experiment verifies the tracking performance, anti-interference capabilities and robustness of the FOPID controller. Thus, the FOPID controller designed in this paper is fit for space teleoperation time-delay system and meets the development direction of future space operation tasks.

Key words: space teleoperation; PID control; fractional calculus; stability domain of controller parameters; D-decomposition method

1 Introduction

Space teleoperation will develop to be “more careful and more flexible” in the future^[1], such as space processing and assembly. Being “more careful” requires the control system to have small overshoot and precise response, and being “more flexible” requires the control system to have fast response, for which the operator does not have obvious sense of time-delay, and the operation will be more flexible.

PID controllers have been widely used in space teleoperation systems, such as the bilateral teleoperation experiment of Japanese ETS-VII^[2], because of the fea-

tures of simple structures, robustness and easy operation. However, the contradiction between short settling time and small overshoot limits the performance of the conventional PID controller. As a result, the conventional PID controller has difficulty in meeting the requirement of being “more careful and more flexible” for space teleoperation.

Because of the continuous integration order λ and differential order μ , the fractional-order PID (FOPID) controller, which was proposed by I. Podlubny^[3] in 1999, is more flexible to choose an appropriate λ and μ to adjust the dynamic performance of the control sys-

Received 22 April 2015; accepted 15 March 2016.

[†]Corresponding author. E-mail: 541390019@qq.com; Tel.: +86 10-66360505.

Recommended by Associate Editor HU Yueming.

Supported by National Natural Science Foundation of China (11402004).

tem. As a result, FOPID controllers can effectively alleviate the contradiction between short settling time and small overshoot, and meet the requirement of being “more careful and more flexible” for space teleoperation.

Parameters tuning is one of the hot topics for FOPID controllers^[4–5]. Rajasekhar A.^[6] designed an optimum FOPID controller for a head positioning servomechanism in a hard disk drive and tuned the controllers for optimal parameters using a new swarm intelligence based on differential search algorithm. Dev D. V.^[7] developed a modified method of tuning for FOPID controllers. It is basically a loop shaping procedure where the frequency response of the system is reshaped. Necaibia A.^[8] proposed to apply the classical PID extremum seeking-based auto-tuning method to adjust the FOPID controller for DC motor speed control. AlMayyahi A.^[9] used particle swarm algorithm to optimize the FOPID controller for overcoming the path tracking problem of autonomous ground vehicles. Ates A.^[10] proposed master-slave optimization approach according to the Bode’s ideal transfer function which is used as a reference model, in order to govern the optimization of FOPID control system. However, there is still no report of a FOPID controller design for space teleoperation time-delay systems.

This paper presents a novel FOPID controller design method for teleoperation of a free-flying space robot based on fractional calculus. The parameters of FOPID controller are tuned based on its stability domain directed at the space teleoperation time-delay system. This paper is organized as follows. Section 2 presents the FOPID control method for space teleoperation, on the basis of the conventional PID control method. Section 3 tunes the parameters of FOPID controller directing at the space teleoperation time-delay system, and discusses the advantages of FOPID control method for space teleoperation. Section 4 presents the simulation results of a comparison between PID controller and FOPID controller. Ground experiment results are showed in Section 5, and Section 6 concludes with the obtained results and outlines the future work.

2 FOPID control principle for space teleoperation

2.1 Model for space teleoperation

The nonlinear dynamic model for a free-flying space robot with n -degrees of freedom can be described as^[11]

$$\mathbf{M}_{\mathbf{q}_r}(\mathbf{q}_r)\ddot{\mathbf{q}}_r + \mathbf{C}_{\mathbf{q}_r}(\mathbf{q}_r, \dot{\mathbf{q}}_r)\dot{\mathbf{q}}_r = \boldsymbol{\tau}_r + \boldsymbol{\tau}_d, \quad (1)$$

where $\mathbf{q}_r, \dot{\mathbf{q}}_r, \ddot{\mathbf{q}}_r \in \mathbb{R}^{n \times 1}$ is the joint angle, velocity and acceleration, respectively; $\mathbf{M}_{\mathbf{q}_r}(\mathbf{q}_r) \in \mathbb{R}^{n \times n}$ is the inertia matrix; $\mathbf{C}_{\mathbf{q}_r}(\mathbf{q}_r, \dot{\mathbf{q}}_r) \in \mathbb{R}^{n \times n}$ is the coefficient matrix of centrifugal, Coriolis and velocity damping; $\boldsymbol{\tau}_r \in \mathbb{R}^{n \times 1}$ is the control torque; and $\boldsymbol{\tau}_d \in \mathbb{R}^{n \times 1}$ is the

disturb torque.

A single rotating joint of the space robot is considered here, and the coupling force among joints is regarded as the disturb torque; therefore, $\mathbf{M}_{\mathbf{q}_r}(\mathbf{q}_r) = J$, $\mathbf{C}_{\mathbf{q}_r}(\mathbf{q}_r, \dot{\mathbf{q}}_r) = C$, $\mathbf{q}_r = \theta$, and the state-space representation of space teleoperation is shown in the following equation:

$$\begin{cases} \dot{\mathbf{X}}(t) = \mathbf{A}\mathbf{X}(t) + \mathbf{B}u(t - \tau_u) + \mathbf{D}\omega(t), \\ y(t) = \mathbf{L}\mathbf{X}(t), \end{cases} \quad (2)$$

where $\mathbf{X} = [x_1, x_2]^T = [\theta, \dot{\theta}]^T$, $u = \tau_r$, $\omega = \tau_d$, $y = x_1 = \theta$, $\mathbf{A} = [0, 1; 0, -C/J]$, $\mathbf{B} = [0, 1/J]^T$, $\mathbf{D} = [0, 1/J]^T$, $\mathbf{L} = [0, 1]^T$, and τ_u is the up-link time-delay of space teleoperation.

According to the analysis of the experimental data from “Space maintenance technology scientific experiments” in China, space environment disturbances, delay jitters, and non-modeling errors, etc. are the main influence factors of the dynamic control for space teleoperation. On the order of magnitude, the joint errors caused by space environment disturbances are about 0.01 rad, delay jitters are about 0.1 s, and the model parameters change caused by non-modeling errors and space environment are about 50%. All of these influence factors have been considered in the simulation experiments in Section 4, and it is necessary to design a controller for space teleoperation.

2.2 Conventional PID control method

The conventional PID control principle for space teleoperation^[12] is shown in Fig.1, where the PID controller is calculated as follows:

$$C(s) = k_p + k_i \frac{1}{s} + k_d s, \quad (3)$$

where k_p , k_i and k_d are the proportional coefficient, integral coefficient and derivative coefficients, respectively.

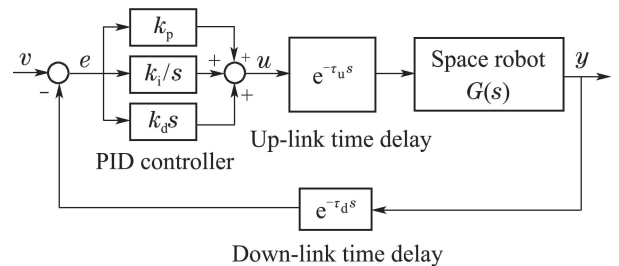


Fig. 1 Conventional PID control principle for space teleoperation

The control variable u is calculated:

$$u = k_p e + k_i \int e dt + k_d \dot{e}, \quad (4)$$

where the state error(e) is calculated as $e = v - y$.

Thus, the closed-loop transfer function of space teleoperation system can be written as follows:

$$G_{cl}(s) = \frac{C(s)G(s)e^{-\tau_u s}}{1 + C(s)G(s)e^{-(\tau_u + \tau_d)s}}. \quad (5)$$

2.3 Application of fractional calculus theory

Fractional calculus theory is the extension of integer calculus, whose integral and derivative order are arbitrary^[13-14]. Based on the fractional calculus theory, the transfer function of POPID controller is

$$C_f = k_p + k_i \frac{1}{s^\lambda} + k_d s^\mu, \quad (6)$$

where λ and μ are the integral and derivative orders, respectively.

Based on fractional calculus, this paper proposes the FOPID control method for space teleoperation that is shown in Fig.2, and the closed-loop transfer function of the space teleoperation system is

$$G_{cl}(s) = \frac{C_f(s)G(s)e^{-\tau_u s}}{1 + C_f(s)G(s)e^{-(\tau_u + \tau_d)s}} = \frac{K(k_i + k_p s^\lambda + k_d s^{\lambda + \mu})e^{-\tau_u s}}{s^{\lambda + 1}(Ts + 1) + K(k_i + k_p s^\lambda + k_d s^{\lambda + \mu})e^{-(\tau_u + \tau_d)s}}, \quad (7)$$

where $K = 1/C$ and $T = J/C$ are the naturalization coefficients.

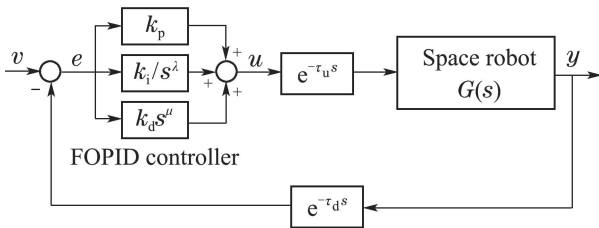


Fig. 2 FOPID control principle for space teleoperation

3 FOPID controller design for space teleoperation

3.1 Parameters tuning of FOPID controller

From formula (7), the closed-loop characteristic equation is

$$P(s; k_p, k_i, k_d, \lambda, \mu) = Ts^{\lambda + 2} + s^{\lambda + 1} + K(k_i + k_p s^\lambda + k_d s^{\lambda + \mu})e^{-(\tau_u + \tau_d)s}. \quad (8)$$

Definition 3.1 The stability domain \mathcal{S} of the FOPID controller parameters is defined as for $(k_p, k_i, k_d, \lambda, \mu) \in \mathcal{S}$ the roots of $P(j\omega; k_p, k_i, k_d, \lambda, \mu) = 0$ all lie in open left-half of the s -plane, which ensures the system keeps stable.

According to the D–decomposition method^[15], the boundaries of \mathcal{S} are composed by the real root boundary (RRB), the infinite root boundary (IRB) and the complex root boundary (CRB).

RRB:

$$P(0; k_p, k_i, k_d, \lambda, \mu) = 0 \Rightarrow k_i = 0. \quad (9)$$

IRB:

$$P(\infty; k_p, k_i, k_d, \lambda, \mu) = 0 \Rightarrow$$

$$\begin{cases} k_d = 0, & \mu > 2, \\ k_d = \pm T/K, & \mu = 2, \\ \text{none}, & \mu < 2. \end{cases} \quad (10)$$

The CRB is constructed by substituting $s = j\omega$:

$$P(j\omega; k_p, k_i, k_d, \lambda, \mu) = R_e + jI_m = 0, \quad (11)$$

where R_e and I_m denote the real and imaginary parts, respectively.

The CRB can be obtained by equating the real and imaginary parts to zero:

$$k_p = \frac{XR - YQ + k_d(KR - LQ)}{ZR - QT}, \quad (12)$$

$$k_i = \frac{YZ - XT + k_d(LZ - KT)}{ZR - QT}, \quad (13)$$

where

$$Z = K\omega^\lambda \cos\left(\frac{\pi}{2}\lambda - \omega(\tau_u + \tau_d)\right),$$

$$T = K\omega^\lambda \sin\left(\frac{\pi}{2}\lambda - \omega(\tau_u + \tau_d)\right),$$

$$Q = K \cos(\omega(\tau_u + \tau_d)),$$

$$R = -K \sin(\omega(\tau_u + \tau_d)),$$

$$K = -K\omega^{\lambda + \mu} \cos\left(\frac{\pi}{2}(\lambda + \mu) - \omega(\tau_u + \tau_d)\right),$$

$$L = -K\omega^{\lambda + \mu} \sin\left(\frac{\pi}{2}(\lambda + \mu) - \omega(\tau_u + \tau_d)\right),$$

$$X = T\omega^{\lambda + 2} \cos\left(\frac{\pi}{2}\lambda\right) + \omega^{\lambda + 1} \sin\left(\frac{\pi}{2}\lambda\right),$$

$$Y = T\omega^{\lambda + 2} \sin\left(\frac{\pi}{2}\lambda\right) - \omega^{\lambda + 1} \cos\left(\frac{\pi}{2}\lambda\right).$$

Then, the parameters of FOPID controller are tuned:

Step 1 (Integral order calculation) Fix $k_d = 1$ and $\mu = 1$, change λ from 0.2 to 1.7, and plot the RRB line, IRB line, and CRB curve on the (k_p, k_i) -plane, as shown in Fig.3. The λ is chosen as the integral order when the stability region was largest.

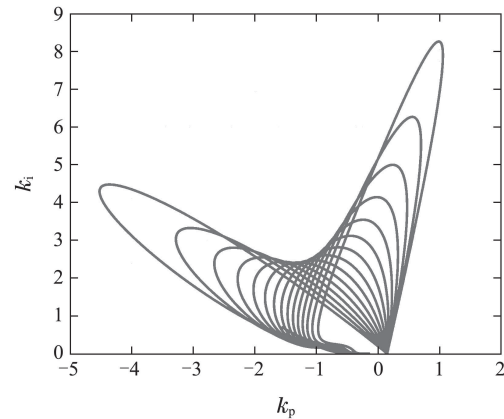


Fig. 3 The stability region of PI^λD controller parameters ($k_d = 1, \mu = 1$, and changing λ from 0.2 to 1.7)

Step 2 (Derivative order calculation) As Step 1, fix $k_d = 1$, and $\lambda = 1$, change μ from 0.2 to 1.7, and plot the RRB line, IRB line, and CRB curve on the

(k_p, k_i) -plane, as shown in Fig.4. The μ is chosen as the derivative order when the stability region was largest.

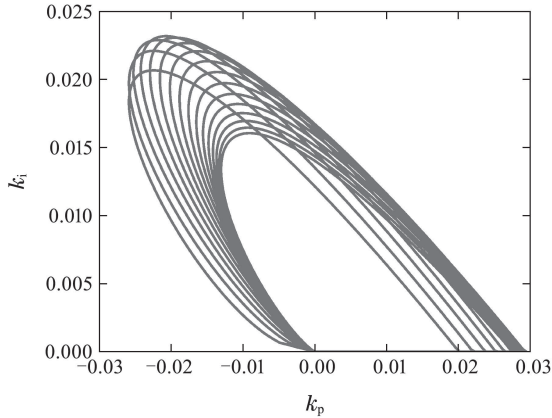


Fig. 4 The stability region of PID^μ controller parameters ($k_d = 1, \lambda = 1$, and changing μ from 0.2 to 1.7)

Step 3 (Virtual magnitude-phase margin tester introduction) Introduce the virtual magnitude-phase margin tester $C_t(A, \varphi) = Ae^{-\varphi}$ into the control system, in order to meet the desired magnitude margin A and phase margin φ , as shown in Fig.5.

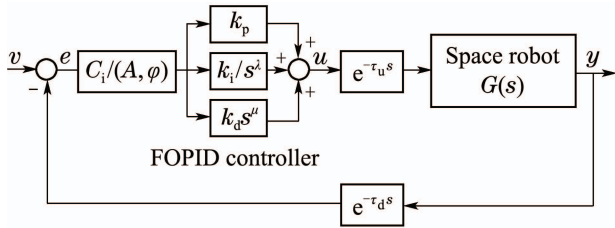


Fig. 5 The principal of FOPID control with magnitude-phase margin tester for space teleoperation

The closed-loop transfer function of this system is

$$G_{cl}(s) = \frac{C_f(s)G(s)e^{-\tau_u s}}{1 + C_f(s)G(s)e^{-(\tau_u + \tau_d)s}} = \frac{K(k_i + k_p s^\lambda + k_d s^{\lambda + \mu})e^{-\tau_u s}}{s^{\lambda + 1}(Ts + 1) + K(k_i + k_p s^\lambda + k_d s^{\lambda + \mu})e^{-(\tau_u + \tau_d)s}}, \quad (14)$$

and the closed-loop characteristic equation is

$$P(s; k_p, k_i, k_d, \lambda, \mu) = Ts^{\lambda + 2} + s^{\lambda + 1} + AK(k_i + k_p s^\lambda + k_d s^{\lambda + \mu})e^{-(\tau_u + \tau_d)s}e^{-j\varphi}. \quad (15)$$

Step 4 (Stability domain calculation) D-decomposition method was used for formula (15) to obtain the stability region of the system parameters.

Step 5 (Coefficient determination) The stability region of the system parameters is the 3-dimensional (k_p, k_i, k_d) -space, since the integral order λ and the derivative order μ are determined. The parameters (k_p, k_i, k_d) can be chosen from this 3-dimensional (k_p, k_i, k_d) -space to meet the specified magnitude and phase margins.

3.2 Advantages of FOPID control method for space teleoperation

Remark 1 The FOPID control method will meet the development direction of future space teleoperation tasks.

The conventional PID control method is based on the idea of error feedback and obtains the control variable by the linear combination of the proportion, integration, and differential of error. However, the integration may increase the settling time of the system and slow the dynamic response, and the differential may amplify the noise and cause oscillation, which has caused difficulties in meeting the requirement of being “more careful and more flexible”. Compared to the conventional PID controller whose integral order and derivative order are 1, the FOPID controller can change the integral order and derivative order arbitrarily, and the parameter tuning method used in this paper can specify the magnitude margin and phase margin of closed-loop system in order to improve the dynamic performance, which will effectively overcome the contradiction between short settling time and small overshoot to meet the requirement of being “more careful and more flexible” for space teleoperation.

The influence of different λ and μ values in a FOPID controller was analyzed in Fig.6 and Fig.7.

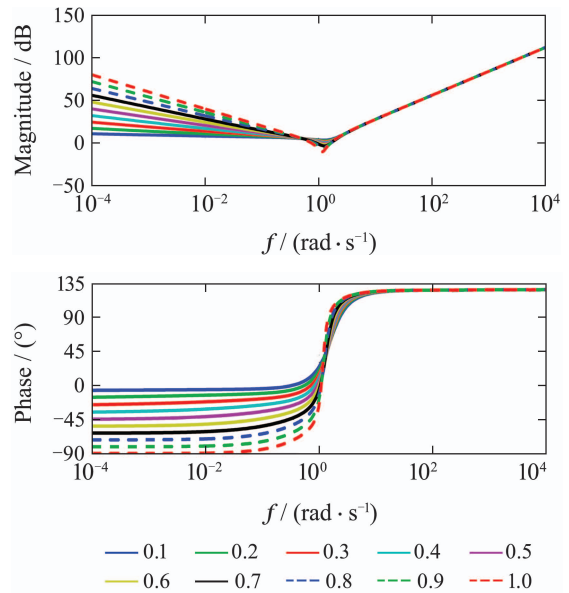
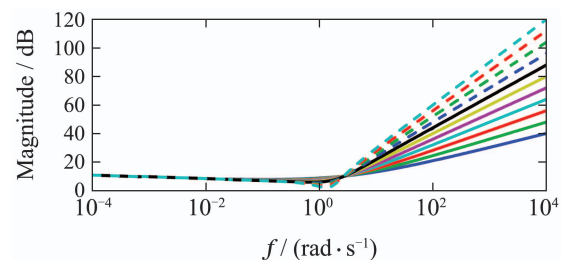


Fig. 6 The Bode diagram of FOPID controller for various λ



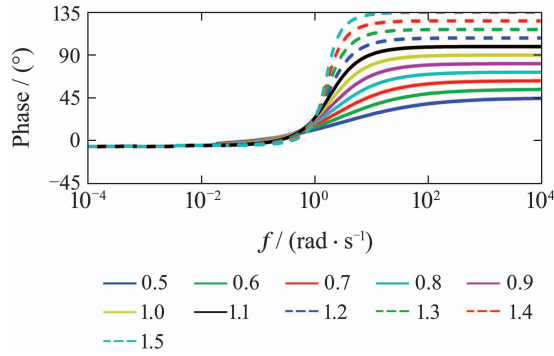


Fig. 7 The Bode diagram of FOPID controller for various μ

From Fig.6, the integral order λ affects the low frequency characteristic of the control system. With the accretion of integral order λ , the integral effect of the control system is enhanced, and the slope of low-frequency curve is increased; therefore, the system peak will increase, and the settling time will be longer. From Fig.7, it can be seen that the derivative order μ affects the mid-frequency characteristic of the control system. With the accretion of derivative order μ , the derivative effect of the control system is enhanced, and the slope of mid-frequency stage for the amplitude-versus-frequency curve becomes gentle, which will make the overshoot smaller and the settling time shorter. However, if the derivative order μ is oversized, the slope of the mid-frequency stage will be cliff-like, and the system will be unstable.

Remark 2 the FOPID controller design method presented in this paper is fit for space teleoperation which is a complex time-delay system and has good capabilities of preventing delay jitters.

The parameter tuning method avoids the errors that result from the rational approximation of time-delay $e^{-(\tau_u+\tau_d)s}$, which is fit for time-delay systems and will eliminate the negative influence caused by delay jitters.

Remark 3 The newly designed FOPID controller will eliminate the negative influence of model parameter changes caused by the space environment.

The largest stability domain for FOPID controller parameters was chosen when tuning the parameters, which increases the robustness of control system to maintain stability when model parameters are changed as a result of space environment.

Remark 4 The FOPID controller has the capability of rejecting the disturbance from space environment.

When the disturbances from space environment are put into the control system, the differential can predict the errors, the integration can eliminate the steady-state errors, and the order is optional to im-

prove the steady-state performance.

4 Simulation results

As a validation of the proposed method, a PID controller and a FOPID controller for space teleoperation are compared in terms of their control performance. The parameters are chose as $J = 0.15 \text{ kg}\cdot\text{m}^2$, $C = 0.05$, $\tau_u = \tau_d = 1.1 \text{ s}$, and the parameters tuning method mentioned in last section is used to get the transfer function for FOPID controller:

$$C_f(s) = 7.2 \times 10^{-3} - \frac{5.3 \times 10^{-4}}{s^{0.2}} + 2.7 \times 10^{-4} s^{1.5}. \quad (16)$$

The design method of optimal PID controller for time-delay system, proposed by Hu T^[16], was used:

$$C(s) = 4.31 \times 10^{-3} + \frac{5.26 \times 10^{-5}}{s} + 1.58 \times 10^{-5} s. \quad (17)$$

4.1 Tracking performance

Two kinds of input, step-input $v = 1 \text{ rad}$ and sine-input $v = \sin(t/30) \text{ rad}$, are considered here, respectively, as Fig.8 and Fig.9 shown, and the comparison results of unit step response are shown in Table 1.

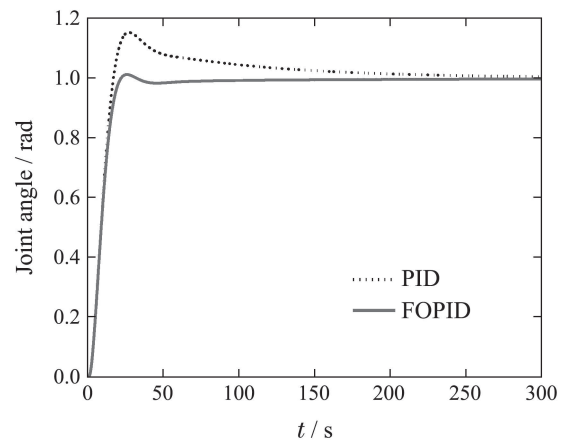


Fig. 8 Unit step response

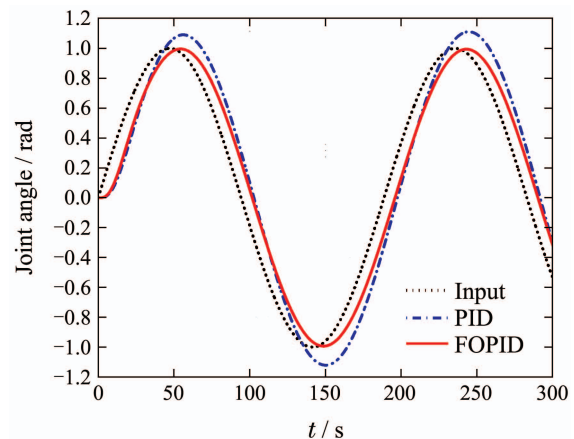


Fig. 9 Sine-input response

Table 1 Comparison of unit step response performance

Controller	Peak time/s	Over-shoot/%	Settling time/s	Steady-state error/%
PID	28.57	15.2	168.6	0
FOPID	25.03	1.19	20.38	0

Simulation results show that, FOPID controller has shorter settling time, shorter rising time and smaller overshoot compared to the PID controller. Therefore, FOPID controller has better tracking performance and will meet the requirement of being “more careful and more flexible” for space teleoperation.

4.2 Anti-interference capabilities

Two kinds of external disturbance, Gaussian random disturbance with a mean of 0 and a standard deviation of 0.01 rad and sinusoidal disturbance $w(t) = 0.1 \sin(0.5t)$, are supposed. Compared to PID controller, the FOPID controller can eliminate the negative influence generated by Gaussian random disturbance and weaken the sinusoidal disturbance (amplitude is weakened from 0.1 rad to 0.01 rad), as shown in Fig.10 and Fig.11.

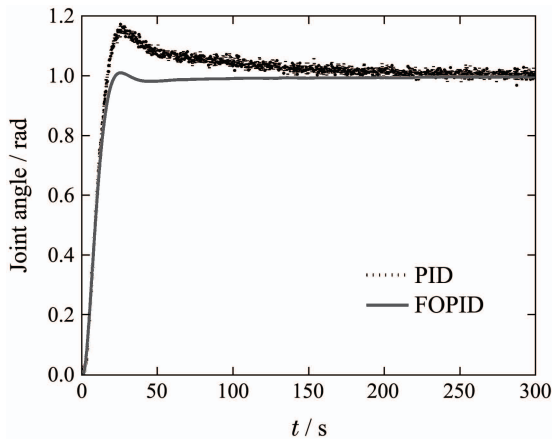


Fig. 10 Step response with Gaussian random disturbance

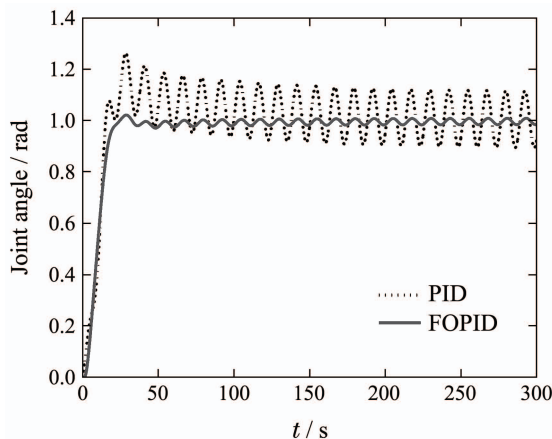


Fig. 11 Step response with sinusoidal disturbance

4.3 Capabilities of preventing delay Jitters

As shown in Fig.12 and Fig.13, a Gaussian random time-delay with a mean of 1.1 s and a standard deviation of 0.1 s is considered. The FOPID control system maintains better tracking performance than PID controller when the time-delay was random, which indicates that FOPID controller has better capabilities of preventing delay jitters.

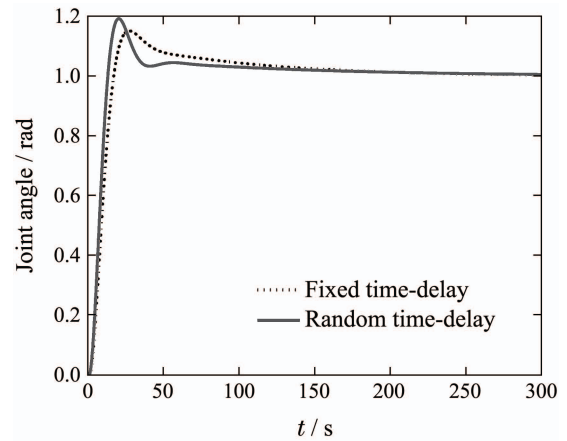


Fig. 12 Step response with random time-delay for PID controller

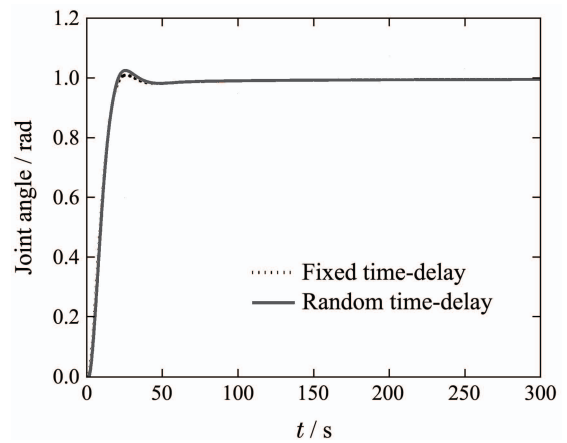


Fig. 13 Step response with random time-delay for FOPID controller

4.4 Robustness

Robustness is studied here by adding 50% model error. The results are shown in Fig.14 and Fig.15, which show that FOPID controller has better robustness than PID controller and can eliminate the negative influence of model error caused by space environment.

5 Ground experiment

A ground experiment verification platform was constructed, as shown in Fig.16, which chose the Joint 2, 3 and 5 of the 6-DOF robot named Googol GRB3016-06 as the controlled object, and the robot has no contract force affected by the environment.

Supposing each link of the manipulator is rigid, the mass is uniform distribution, and the centroid is located in the center of each link. In addition, regardless of the cross-sectional size, each link is viewed as a line with mass only, to form the planar 3-DOF serial link manipulator as shown in Fig.17 with the dynamic parameters as follows: 1) Link length: $a_1 = 0.985$ m, $a_2 = 0.765$ m, $a_3 = 0.390$ m; 2) Link mass: $m_1 = 67.5$ kg, $m_2 = 61.0$ kg, $m_3 = 11.9$ kg; 3) Moment of inertia: $I_i = m_i a_i^2 / 12$; 4) Damping coefficient of each link: $C = 0.05$.

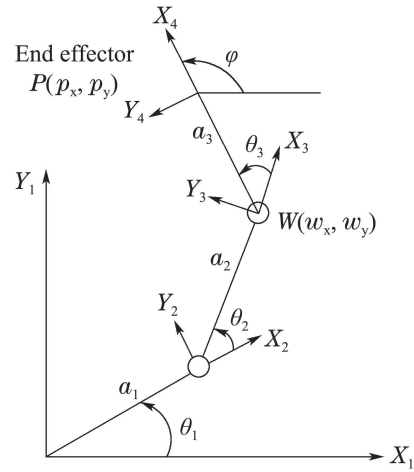


Fig. 17 3-DOF serial link manipulator

The up-link and down-link time-delay of teleoperation system is between 1.05 s and 1.2 s, with a jitter of 0.15 s. In the experiment, the operator controlled the telerobot to complete the arc trajectory tracking task using a hand controller, and conventional PID and FOPID controllers were designed to generate the control command. The telerobot's end effector trajectory, controlled by PID and FOPID controllers, respectively, are shown in Fig.18, and the tracking error of relative position and the error of the three joints are shown in Fig.19 and Fig.20, respectively.

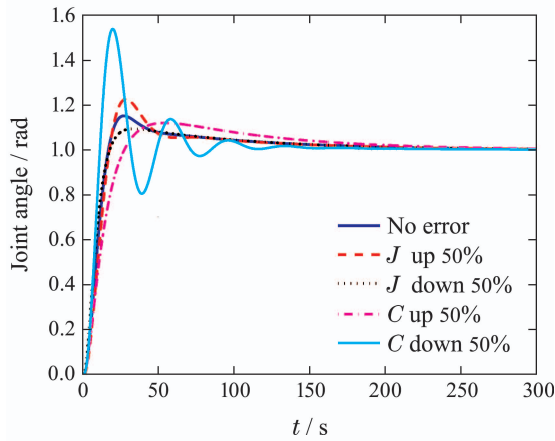


Fig. 14 Step response with model error for PID controller

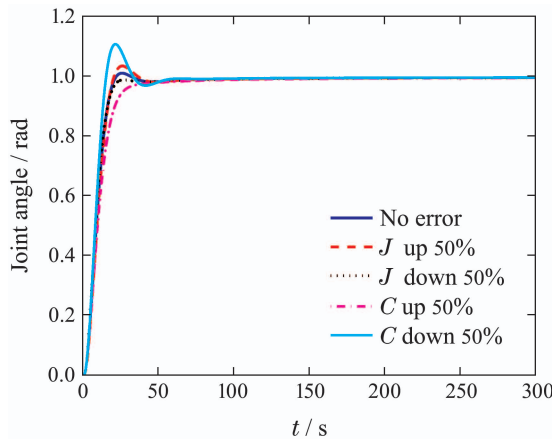


Fig. 15 Step response with model error for FOPID controller

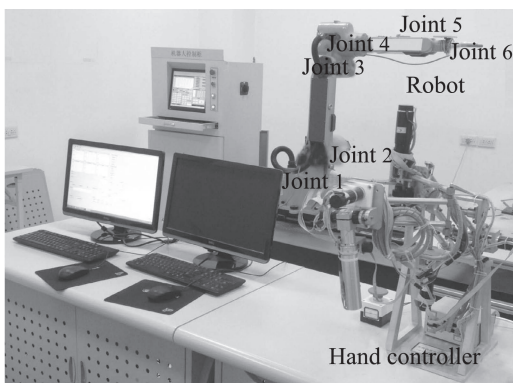


Fig. 16 Ground experiment verification platform for teleoperation system

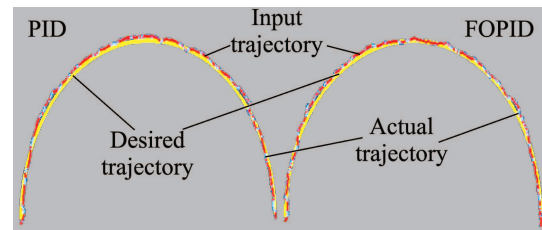


Fig. 18 The robot's end effector trajectory controlled by PID and FOPID controller

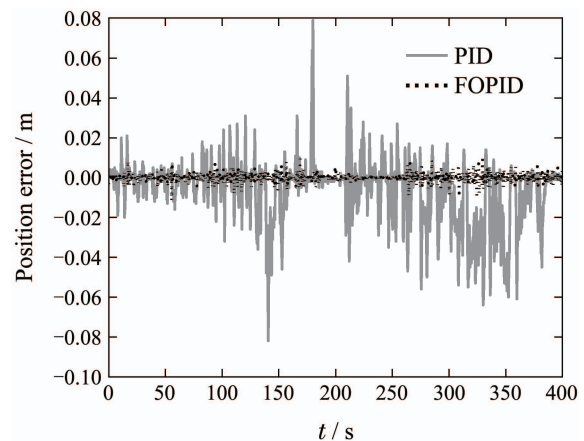


Fig. 19 Tracking error of end effector trajectory

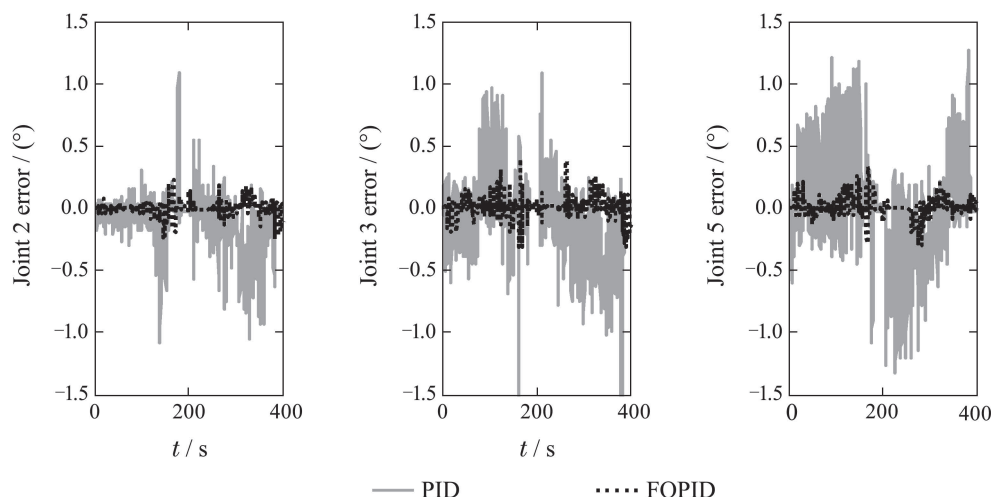


Fig. 20 Control error of three joints

From Fig.19, the tracking error of relative position for FOPID controller was about 0.01 m, which was smaller than PID controller's tracking error of about 0.08 m. Based on Fig.20, the control error of the three joints for the FOPID controller was about 0.5° , which is much smaller than PID controller's control error of about 1.5° . As a result, the FOPID control method proposed in this paper can further effectively overcome the negative influence of model error, time-delay and delay jitters compared to the conventional PID control method. Therefore, the FO PID controller is more suitable for future space teleoperation tasks.

6 Conclusions

This paper has studied the FOPID control method for teleoperation of a free-flying space robot, and tuned the parameters of FOPID controller based on the stability domain of the system parameters directed at the space teleoperation time-delay system. The experimental results show that, compared to the conventional PID controller, the FOPID controller is better at tracking performance, anti-interference capabilities and robustness, which indicates that the FOPID control method is fit for space teleoperation time-delay system and meets the development direction of future space operation tasks.

Reference:

- [1] HUANG Panfeng, LIU Zhengxiang. *Space Teleoperation Technology* [M]. Beijing: National Defense Industry Press, 2015. (黄攀峰, 刘正雄. 空间遥操作技术 [M]. 北京: 国防工业出版社, 2015.)
- [2] IMAIDA T, YOKOKOHI Y, ODA M. Ground-space bilateral teleoperation of ETS-VII robot arm by direct bilateral coupling under 7-s time delay condition [J]. *IEEE Transactions on Robotics and Automation*, 2004, 20(3): 499 – 511.
- [3] POLUBNY I. Fractional-order systems and $PI^\lambda D^\mu$ controllers [J]. *IEEE Transactions on Automatic Control*, 1999, 44(1): 208 – 214.
- [4] ZHU Chengxiang, ZOU Yun. Summary of research on fractional-order control [J]. *Control and Decision*, 2009, 24(2): 161 – 169. (朱呈祥, 邹云. 分数阶控制研究综述 [J]. 控制与决策, 2009, 24(2): 161 – 169.)
- [5] XUE Dingyu, ZHAO Chunna. Fractional order PID controller design for fractional order system [J]. *Control Theory & Applications*, 2007, 24(5): 771 – 776. (薛定宇, 赵春娜. 分数阶系统的分数阶PID控制器设计 [J]. 控制理论与应用, 2007, 24(5): 771 – 776.)
- [6] RAJASEKHAR A, PANT M, ABRAHAM A. Differential search algorithm based design of fractional order PID controller for hard disk drive read/write system [C] // *Proceedings of IEEE International Conference on Systems, Man, and Cybernetics*. Mancheste: IEEE, 2013, 2019 – 2025.
- [7] DEV D V, KUMARI S U. Modified method of tuning for fractional PID controllers [C] // *Proceedings of International Conference on Power Signals Control and Computations*. Thrissur: IEEE, 2014, 1: 1 – 6.
- [8] NECAIBIA A, ABDELICHE F, LADACI S. Optimal auto-tuning of fractional order $PI^\lambda D^\mu$ controller for a DC motor speed using Extremum seeking [C] // *Proceedings of International Conference on Fractional Differentiation and Its Applications*. Catania: IEEE, 2014, 1 – 6.
- [9] ALMAYYAH A, WANG W, BIRCH P. Path tracking of autonomous ground vehicle based on fractional order PID controller optimized by PSO [C] // *Proceedings of IEEE International Symposium on Applied Machine Intelligence and Informatics*. Herl'any: IEEE, 2015, 109 – 114.
- [10] ATEs A, YEROGU C, ALAGOZ B B. Tuning of fractional order PID with master-slave stochastic multi-parameter divergence optimization method [C] // *Proceedings of International Conference on Fractional Differentiation and Its Applications*. Catania: IEEE, 2014, 1 – 6.
- [11] YU Zhigang, SHEN Yongliang, SONG Zhongmin. Robust adaptive motion control for manipulator [J]. *Control Theory & Applications*, 2011, 28(7): 1021 – 1024. (于志刚, 沈永良, 宋中民. 机械臂鲁棒自适应控制 [J]. 控制理论与应用, 2011, 28(7): 1021 – 1024.)
- [12] HU T, HUANG X, TAN Q. Error feedback controller for autonomous space teleoperation [J]. *Procedia Engineering*, 2012, 29(1): 1142 – 1149.
- [13] KENNETH S, MILLER, ROSS B. *An Introduction to the Fractional Calculus and Fractional Differential Equations* [M]. New York: Wiley, 1993.

- [14] CAO Junyi, CAO Binggang. Digital realization and characteristics of fractional order controllers [J]. *Control Theory & Applications*, 2006, 23(5): 791 – 794.
(曹军义, 曹秉刚. 分数阶控制器的数字实现及其特性 [J]. *控制理论与应用*, 2006, 23(5): 791 – 794.)
- [15] HAMAMCI S E. An algorithm for stabilization of fractional-order time delay systems using fractional-order PID controllers [J]. *IEEE Transactions on Automatic Control*, 2007, 52(10): 1964 – 1969.
- [16] HU T, HUANG X, HUANG J. Optimal PID control for time-delay system [C] // *Proceedings of International Conference on Information, Electronics and Computer Science*. Tianjin: IEEE, 2011, 315 – 318.

作者简介:

时 中 (1991–), 男, 硕士研究生, 主要从事空间遥操作控制方法研究, E-mail: 541390019@qq.com;

黄学祥 (1970–), 男, 研究员, 主要从事空间操控技术研究, E-mail: h_xxiang@163.com;

谭 谦 (1972–), 男, 副研究员, 主要从事空间遥操作技术研究, E-mail: tanqian@163.com;

胡天健 (1987–), 男, 博士研究生, 主要从事动力学与控制研究, E-mail: htj13@mails.tsinghua.com.cn.